

Structure and infrared spectra of hydrocarbon interstellar dust analogs

Germán Molpeceres, Vicente Timón, Miguel Jiménez-Redondo, Rafael Escribano, Belén Maté, Isabel Tanarro and Víctor J. Herrero

Instituto de Estructura de la Materia, IEM-CSIC, Serrano 123, 28006 Madrid, Spain

Abstract

A theoretical study of the structure and mid infrared (IR) spectra of interstellar hydrocarbon dust analogs is presented, based on DFT calculations of amorphous solids. The basic molecular structures for these solids are taken from two competing literature models. The first model considers small aromatic units linked by aliphatic chains. The second one assumes a polyaromatic core with hydrogen and methyl substituents at the edges. The calculated spectra are in reasonably good agreement with those of aliphatic-rich and graphitic-rich samples of hydrogenated amorphous carbon (HAC) generated in our laboratory. The theoretical analysis allows the assignment of the main vibrations in the HAC spectra and shows that there is a large degree of mode mixing. The calculated spectra show a marked dependence on the density of the model solids, which evinces the strong influence of the environment on the strengths of the vibrational modes. The present results indicate that a current procedure of estimating the hydrogen and graphitic content of HAC samples through a decomposition of IR features into vibrational modes of individual functional groups is problematic owing to the mentioned mode mixing and to the difficulty for assigning reliable and unique band strengths to the various molecular vibrations. Current band strengths from the literature might overestimate polyaromatic structures. Comparison with astronomical observations suggests that the average structure of carbonaceous dust in the diffuse interstellar medium lies probably in between those of the two models considered, though closer to the more aliphatic structure.

1. Introduction

There is already a large amount of bibliography on the subject of carbon-containing grains in the diffuse interstellar medium (ISM) and in carbon-rich galaxies (see for instance Jones *et al.*,¹ Chiar *et al.*² and references cited therein). This abundance of literature bears witness of the interest of this topic, which is in fact far from being fully interpreted yet. Observational data are mainly IR spectra, from space missions like the Infrared Space Observatory (ISO) or the Spitzer Space Telescope, or from ground based telescopes like the United Kingdom Infrared Telescope (UKIRT). The presence of carbonaceous dust has been inferred from an absorption feature in lines of sight toward sources in the galactic center appearing at 3.4 μm ($\approx 2950 \text{ cm}^{-1}$). This feature typically shows a complex multiple structure, where the components are frequently associated to C-H stretching vibrations of $-\text{CH}_2$ or $-\text{CH}_3$ groups, often accompanied by a peak at 3.3 μm , assigned to aromatic C-H. Absorption bands in the 6 to 8 μm region of the spectra are also evident, and are attributed to bending vibrations of these modes, plus to other modes like C=C or C=O in some cases. The full identification of these observations can only be achieved by comparison to laboratory spectra of molecular species of similar composition to the galactic samples. Predictions from theoretical models can be of great help in the analysis of the observed spectra as well.

As early as 1983 Duley and Williams³ comparison of the observed 3.4 μm band with laboratory data suggested that hydrogenated amorphous carbon was a major component of interstellar dust in diffuse clouds and this material was soon introduced in models of carbonaceous grain evolution in the ISM.⁴ The denomination “hydrogenated amorphous carbon”, usually abbreviated HAC or a-C:H, refers to a wide group of carbonaceous solids with varying proportions of sp^2 and sp^3 hybridized carbon atoms, and different C/H ratios, spanning a range of physical properties intermediate between those of diamond, graphite and polymeric hydrocarbons.⁵⁻⁸ These solids constitute three dimensional structures comprising aromatic islands of variable sizes linked by aliphatic chains, with possible olefinic contributions. In general, the more energetic the formation conditions, the lower the H content and the C sp^3/sp^2 ratio.

Interstellar dust analogs based on amorphous carbon structures are built in the laboratory using various techniques and precursors,⁹ including laser ablation of graphite, laser pyrolysis of a precursor gas,¹⁰ UV irradiation of condensed hydrocarbons,¹¹ or plasma enhanced chemical vapor deposition (PECVD) of gas phase hydrocarbons.^{12,13} The predominant nature of the HAC material in the dust grains of the diffuse ISM is at present a matter of debate between two competing models. In the first of these models, the structure is supposed to be formed by small aromatic islands (typically two benzene rings) linked by aliphatic chains, with possible olefinic inclusions.^{11,14,15} The other model assumes a larger graphitic structure, with small aliphatic contributions.^{16,2} We may refer to these two models as RC (rings + chains) and SG (substituted graphite), respectively, for simplicity. In principle both models have the same functional groups and could offer reasonable explanations for the observed spectra.

The elucidation of the aromatic vs aliphatic content of the carbonaceous dust grains is crucial for chemical models of the cycle of carbon in the ISM.^{2,1} In particular the possible connection between polycyclic aromatic hydrocarbons (PAHs), that display also IR features in the regions

mentioned above, is a matter of current interest. At present, it is argued whether PAHs and HAC are coexisting in some astronomical media, or they represent two phases of the evolutionary stage of one single carbonaceous material.

We present in this work a combined study of laboratory generation and analysis of HAC samples, with the theoretical development of quantum chemical models for analogous amorphous structures, and compare experimental and predicted spectra, trying to infer conclusions on the structure of the samples. In a second stage, we take the results of the theoretical models to analyze the validity of an IR band profile decomposition procedure currently used in the literature for the derivation of the atomic composition of HAC samples. The astrophysical implications of the conclusions of this work are finally discussed.

2. Theoretical models

All our theoretical models have been designed using density functional theory (DFT), which is generally accepted as a good compromise between accuracy and computing cost for solid state materials.¹⁷ The Amorphous Cell code¹⁸ has been used in the generation of the sample unit cells. This code places molecular units in a cell using a Montecarlo algorithm, minimizing inter- and intramolecular close contacts between molecules. In this work a single molecular unit was placed inside a cubic cell whose size was adjusted to yield a target density. Different densities were tested in order to determine the most stable structure and for the comparison of the predicted spectra to experimental observations. Basic units for the RC and SG models were taken from Dartois *et al.*¹¹ and Steglich *et al.*,¹⁶ respectively. They are shown in Fig. 1. The RC basic unit was generated by Dartois *et al.*¹¹ by comparing neuronal network simulations of spectra of model structures with IR absorptions in the diffuse ISM. The SG basic unit corresponds to the average molecular structure of dust grains advanced by Steglich *et al.*,¹⁶ which is based on a thorough investigation combining infrared spectra and theoretical calculations on a large group of individual PAHs and mixtures, and intends to account both for the IR features and for the ultraviolet bump at 217.5 nm observed also in the diffuse ISM.

The structure inside the cell was optimized using CASTEP,^{19,20} a plane wave pseudopotential method, until convergence is achieved, at which position atomic forces and charges were evaluated to finally predict the harmonic vibrational spectrum. For the optimization process with CASTEP, the generalized gradient approximation (GGA) was chosen with the PBEPBE exchange-correlation functional.²¹ A 680 eV energy cutoff for the plane wave expansion has been used in our calculations, along with norm conserving atomic pseudopotentials. The Grimme DFT-D2 correction was also applied.²² The convergence criteria were set at 1×10^{-5} eV/atom for the energy, 0.03 eV/Å for the interatomic forces, and 0.001 Å for the displacements. Good convergence was achieved in all cases. It may be stressed that the calculated spectrum consists of wavenumber and intensity of all fundamental vibrations. All predicted spectra for the RC and SG models calculations reproduced in our figures have been broadened using Gaussian functions of 40 cm^{-1} full width at half maximum (FWHM), to make comparisons easier. Also, for large molecular systems like those in our cells, many vibrations involve motions of several atoms or atomic groups, and it is often difficult to propose a single assignment for each mode.

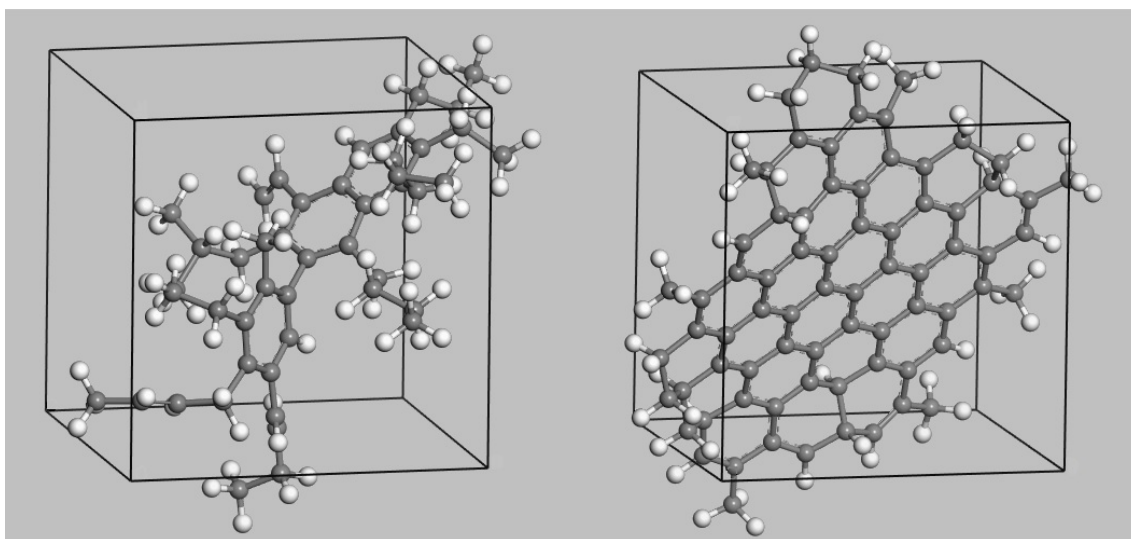


Fig. 1 Models of the two types of structures considered. Left panel: Rings and Chains (RC) model, based on the basic structure proposed by Dartois *et al.*¹¹ Right panel: Substituted graphite model (SG), based on the basic structure suggested by Steglich *et al.*¹⁶ Density of 0.7 g cm^{-3} and 1 g cm^{-3} , respectively. These densities yield the minimum energy structures (see text and Table 2). The drawn cell is shifted along the a, b, c axis of the lattice to better enclose the molecular structures for clarity in the representation.

To assess the validity of our theoretical method, we performed several tests on large molecular systems of known geometry and spectrum, like several PAHs. We found the results satisfactory. As an example, we present in Fig. 2 the case study on the phenanthrene species. The experimental spectrum of crystalline phenanthrene, taken from the NIST database²³ (panel (a) of Fig. 2) is compared with the theoretical spectrum calculated with our approach (panel (b) of Fig. 2). For this comparison, the calculated vibrational frequencies have been represented with Gaussian functions with a FWHM of 8 cm^{-1} , which seems appropriate for the narrow absorption features of the crystalline solid. As can be seen, the global spectrum and most of the experimental vibrational frequencies are well reproduced in the calculations. Besides, the intensity ratio between the most intense peaks in the spectral region below 1000 cm^{-1} , corresponding to aromatic CH bending modes, and that of the less intense band at $\approx 3000 \text{ cm}^{-1}$, associated with CH stretching vibrations, is well accounted for by the theoretical approach. There are however some differences in the peak intensities.

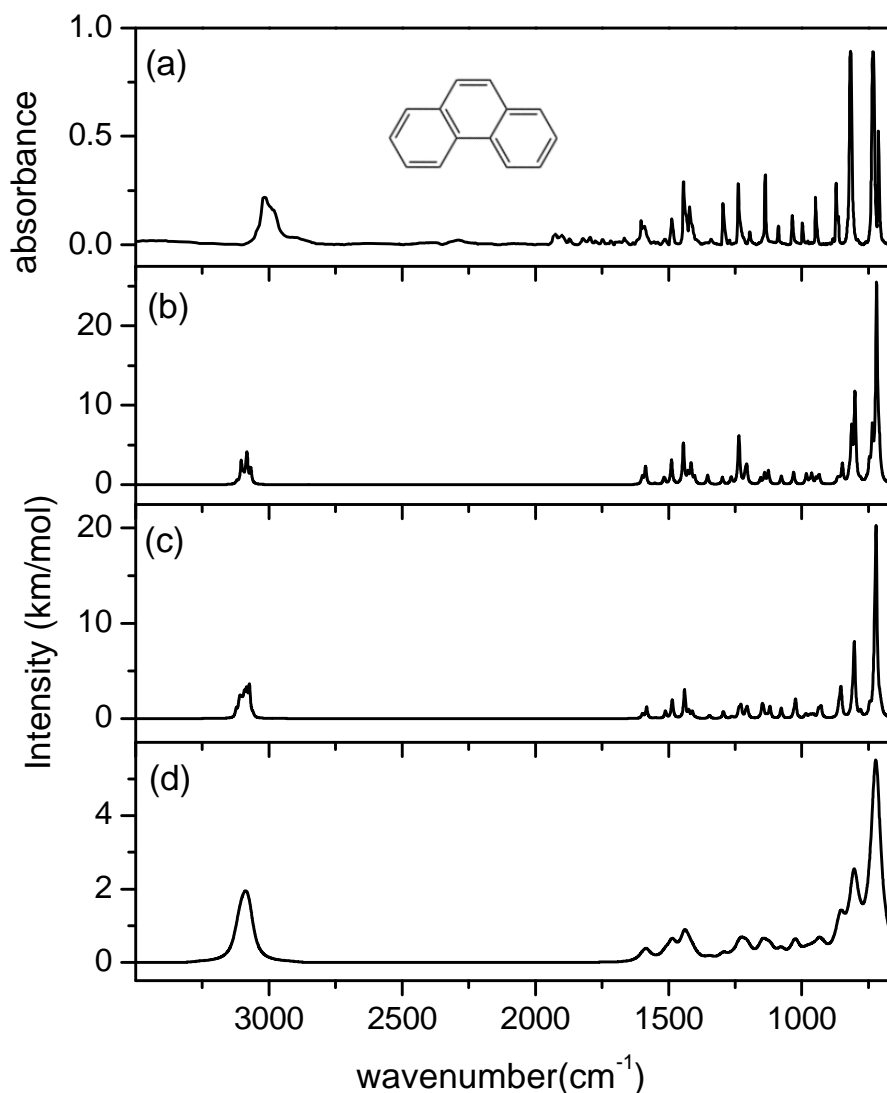


Fig. 2 IR spectra of solid phenanthrene. (a): Experimental spectrum of crystalline phenanthrene, from the NIST database.²³ (b): Calculated spectrum of crystalline phenanthrene represented using Gaussian functions of 8 cm^{-1} FWHM. (c) and (d): calculated spectrum of amorphous phenanthrene represented using Gaussian functions of 8 cm^{-1} and 40 cm^{-1} FWHM, respectively.

In panels (c) and (d) of Fig. 2, we represent the calculated spectrum of amorphous phenanthrene obtained through the amorphization process described above and placing three phenanthrene molecules in a cell to match a density of 1 g/cm^3 . No published spectrum of amorphous phenanthrene seemed to be available. In panel (c) the calculated frequencies are broadened with Gaussians of 8 cm^{-1} FWHM, to allow for a direct comparison with the crystalline calculations of panel (b), and in panel (d) a more realistic spectrum for an amorphous solid is presented using Gaussian functions of 40 cm^{-1} FWHM. Comparison of the panels (b) and (c) shows that there are some changes between the spectrum of the crystalline

and amorphous phases, which could probably be anticipated from the breaking of the symmetry of the crystal causing the splitting of otherwise degenerate modes into several components, mainly in the C-H stretch region around 3100 cm^{-1} .

3. Experimental

Plasma enhanced chemical vapor deposition (PECVD) was used for the production of HAC samples with IR spectra comparable to those of the theoretical RG and SG models. The experimental set-up was described in our earlier publications.^{13,24} It consists of a Pyrex tube (30 cm length, 4 cm diameter) with a 10 turns Cu coil, placed externally around the central part of the tube and fed by a 13.56 MHz RF generator (Hüttinger PFG 300 RF+ matchbox PFM 1500A) which was kept at a constant power of 40 W. Mixtures of CH_4 (5 sccm) and He (10 sccm) were introduced into the reactor up to a pressure of 0.3 mbar. Typical residence times were ≈ 3 s. The HAC deposits were formed on IR transparent substrates (Si or ZnSe) of 2.5 cm diameter, and the normal incidence IR transmission spectra of the deposited samples were then recorded ex-situ with a Bruker Vertex-70 FTIR spectrometer. The spectra were co-added from 250 runs at a nominal resolution of 4 cm^{-1} .

The characteristics of plasma generated HAC samples are known to be dependent on the discharge properties (see for instance Schwarz-Selinger *et al.*²⁵ or Robertson⁸ and references therein). In the present work we have used “soft” deposition conditions to generate hydrogen-rich HAC, with a comparatively high aliphatic content (hereafter S1), and “harsh” deposition conditions for the production of a more graphitic, hydrogen-poor HAC (hereafter S2). Specifically, for the deposition of S1 the substrate was placed outside the coil, 5 cm downstream in the flow direction, and the deposition time was 8 min. For the production of S2 the substrate was kept during 30 min inside the coil and the resulting deposit was further processed in pure H_2 plasma for another 10 min. These conditions, selected after several trials, were found to yield HAC deposits with IR spectra in reasonably good agreement with those of the model calculations.

4. Results

4.1. IR spectra and band assignment

Experimental and theoretical spectra are compared in Fig. 3 and the theoretical assignment of the main molecular vibrations corresponding to the absorption bands is presented in Table 2. In all cases, the spectra are characterized by an absorption maximum in the region ≈ 3000 - 2900 cm^{-1} corresponding to CH stretching modes of CH_3 , CH_2 and CH groups, and by further absorption features in the 1700 - 750 cm^{-1} range due to bending modes of the same groups, as well as to CC and C=C stretch vibrations of the aromatic and olefinic carbon atoms.

On the upper panels of Fig. 3, we show experimental spectra of the S1 and S2 samples. The bending region is prominent in the second one. Below the experimental spectra, we display predicted spectra for the two models used here, that with rings and chains (RC) on the left, and the graphitic-rich (SG) one on the right, for densities of 0.7 g cm^{-3} and 1 g cm^{-3} , respectively. The agreement between observed and calculated spectra seems reasonable in both cases, in terms of wavenumbers and intensity ratios between the CH stretching and

bending zones of the spectra. From the known structure of our models, we conclude that whereas the S1 deposit, generated outside the coil, probably contains small rings and hydrocarbon chains, the S2 sample, produced inside the coil and processed in a H₂ plasma, has a large graphitic content. Thus, the use of our theoretical models and their spectra seems to offer a good tool to investigate the nature of observed HAC samples.

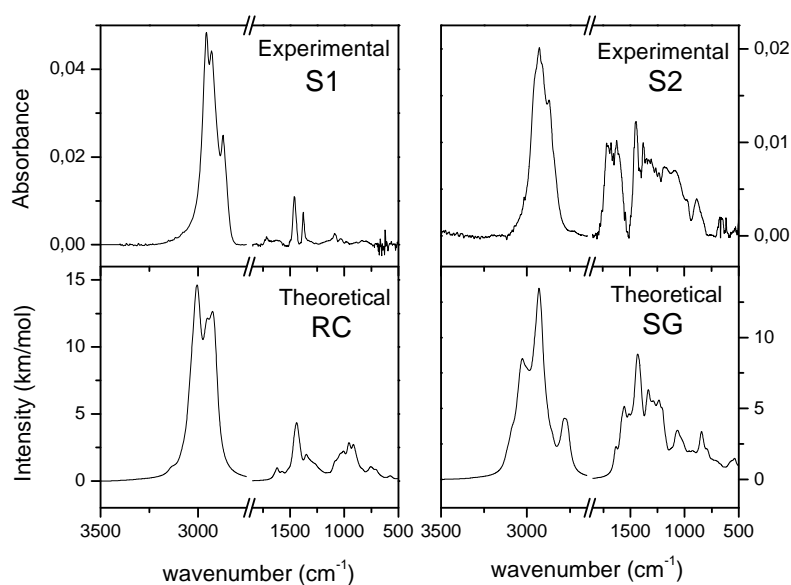


Fig. 3 IR spectra of HAC samples. Upper panels: left, experimental S1 deposit formed outside the coil; right, experimental S2 deposit formed inside the coil with additional H₂ plasma processing. Lower panels: left, Rings and Chains (RC) model for density of 0.7 g cm⁻³; right, Substituted Graphite (SG) model for density of 1 g cm⁻³. These densities correspond to the minimum energy structures.

The theoretical calculations are also very useful to assign the spectra, as they provide a graphical representation of the atomic displacements for each normal mode. However, with large systems as those studied here, we often find modes which involve the motion of several atoms or even atomic groups for the same vibration, and sometimes it is not possible to propose individual assignments, something which is particularly true for the lower frequency modes. Based on our calculations, we have listed in Table 1 the assignment of the main bands observed in the spectra of Fig. 3. This information is especially relevant for the zone below 1500 cm⁻¹, where the assignments are less obvious.

Table 1 Assignments of main vibrations in the HAC spectra of Fig. 3.

Wavenumber range (cm ⁻¹)	RC model	Wavenumber range (cm ⁻¹)	SG model
	Predominant vibrations ^a		Predominant vibrations
3130-3040	CH stretch aromatic, CH ₂	3140-3080	CH stretch, aromatic

	stretch olefinic		
3040-2970	CH ₃ a-stretch, CH ₂ a-stretch	3080-2980	CH ₃ a-stretch, CH ₂ a-stretch, CH-stretch aromatic
2970-2940	CH ₂ a-stretch, CH ₂ s-stretch	2980-2830	CH ₂ s-stretch, CH ₃ s-stretch
2940-2830	CH ₃ s-stretch, CH ₂ s-stretch	2830-2700	CH stretch, tertiary carbon
1650-1590	C=C olefinic	1690-1520	CC stretch, C=C stretch aromatic
1590-1500	C=C stretch aromatic	1520-1370	CH ₃ a-bend+ CH ₂ bend + CH bend
1500-1380	CH ₃ a-bend + CH ₂ s-bend	1370-1300	CH ₃ s-bend
1380-1290	CH ₃ s-bend	1300-1150	CH ₂ bend +CH bend aromatic + CH bend tertiary C
1290-1150	CH ₂ bend	1150-950	CH in plane bend aromatic, CH bend ternary C+ CH ₂ bend
1150-980	CH+CH ₂ +CH ₃ bends	950-750	CH out-of-plane bend aromatic
980-790	CH out-of-plane bend aromatic + CH ₃ bend		

^a Prefix a- and s- indicates asymmetric and symmetric modes, respectively.

In the comparison of experimental and calculated spectra there appear always some zones where a good agreement is never totally reached. In particular, the experimental region of the C-H stretchings around 3000 cm⁻¹ presents a certain profile which changes from S1 to S2. This profile is sometimes decomposed into several components assigned to different CH₂ or CH₃ vibrations (see below for discussion on this). In the calculated spectra, the profile also changes from one model to another, but the calculated relative intensities of the component peaks do not match the observations. The closest case is for S1 and the RC model, but even in this situation a perfect match is not achieved. It may be that the relative number of CH₂ to CH₃ bonds is critical for that aim, but it must be born in mind as well that the calculated intensities, and to some extent the frequencies, of these modes depend markedly on the environment surrounding the bonds, and the intensity of some CH₂ or CH₃ stretching modes can be altered by other nearby bonds or molecules. Also, in the SG spectrum, the peak at 2700 cm⁻¹, which is absent in the experimental S2 spectrum, is almost exclusively due to CH vibrations of diamond-like tertiary carbons. This type of substructure was included by Steglich *et al.*¹⁶ in their model in order to account for a peak initially reported in the observation of some interstellar grains in dense clouds.²⁶ Other conflicting zone in the RC spectrum occurs between 1150 and 790 cm⁻¹ with no clear counterpart in the experimental spectrum of S1. In any case, we cannot expect an exact reproduction of the structure of the matter with the models being used.

4.2. Effects of density

The density of a sample is often a critical unknown when trying to model a solid, especially for amorphous samples. This is particularly so in the present investigation, where this information is poorly known for HAC materials, either fabricated in the lab or studied from astrophysical media. To tackle this problem, we have built series of models of varying density, to select the cases where the predicted spectra are closer to those of the experimental samples.

We reproduce in Fig. 4 calculated spectra of the RC and SG models shown in Fig. 1 for densities from 0.7 g cm⁻³ to 2 g cm⁻³. Densities are determined by choosing the appropriate size of the

cell. Whereas spectra for the two lowest density values do not change very much, those for the highest values show very large alterations, and do not resemble any spectra that we have seen of HAC materials. In the spectra of the 1.5 g cm^{-3} samples, the $1700\text{-}800 \text{ cm}^{-1}$ region, which embraces the angle bendings involving aliphatic CH and the C=C stretchings (see above), is too strong compared to the CH stretchings region, from 3300 cm^{-1} to 2800 cm^{-1} . The intensity ratio between these zones is even farther away from observations for the 2 g cm^{-3} samples, especially in the SG model where a remarkably intense peak at $\approx 2700 \text{ cm}^{-1}$ is evident. This vibration is a C-H stretch large amplitude mode where the H atom is projected away from a C atom of diamond-like configuration, bound to three other C atoms in a pyramidal way, towards a C=C bond of a nearby molecular fragment. The positive charge carried by the proton seems to interact with the high electronic cloud around the C=C bond giving rise to a very large dipole change for the whole structure. This effect bears some similitude with large amplitude vibrations of H-bond systems, where the large intensity is accompanied by a very broad bandwidth in observed spectra, an effect that is not predicted from our calculations. For these amorphous samples of large density, interactions with neighbor molecules become very relevant, even if the structure of each individual molecule is not much altered from that in the isolated species or in low density samples. Other effects observed for increasing density can be noticed in the relative intensities of individual modes within the C-H stretching bundle.

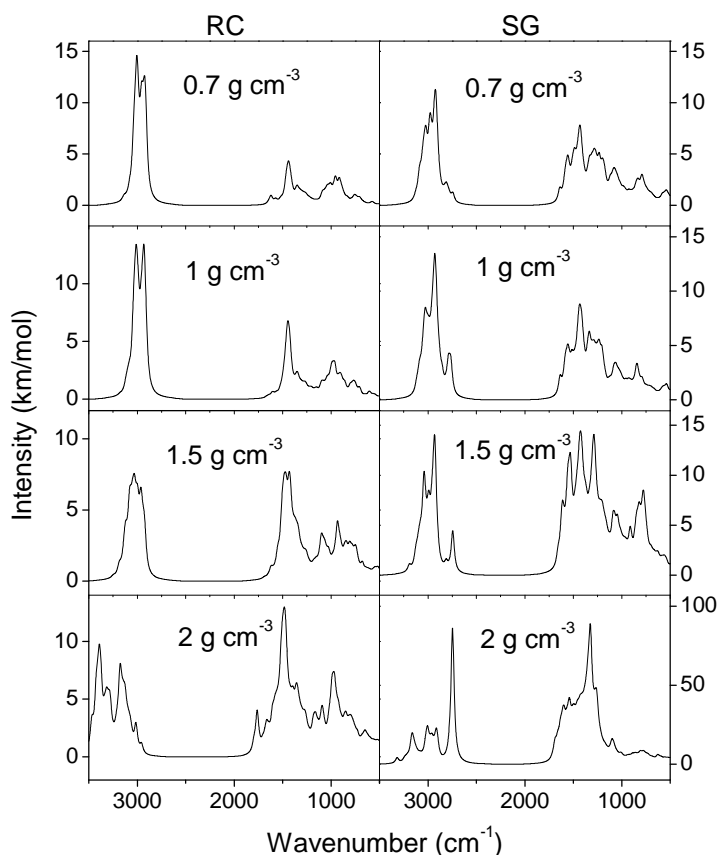


Fig. 4 Calculated IR spectra as a function of density for the two models considered.

At the end of the optimization process, the resulting energy is also an indication of the stability of the sample. For the structures whose spectra are shown in Fig. 4, we list in Table 2 the

increase in energy, ΔE , with respect to the most stable configuration, which for the RC model is that of 0.7 g cm^{-3} and for the SG model, that of 1 g cm^{-3} . The ΔE values are comparable for the lowest density samples, but they increase sharply for the 2 g cm^{-3} and 3 g cm^{-3} species (the latter not shown in Fig. 4). The magnitude of the intermolecular interactions between molecules of the neighboring cells account for the anomalous increase in energy for the higher energy samples. The electronic energy of these structures is therefore dominated by these interactions, pointing out that higher densities lead to excessively compressed incorrect structures.

Although the precise density of the experimental HAC samples is not known, current literature estimates for this type of materials are in the $\approx 1\text{-}2 \text{ g cm}^{-3}$ range,⁸ depending on the hydrogen content. In our calculations, the structures of minimum energy are those which yield the best agreement with the experimental spectra, shown in Fig. 3.

Table 2. Energy increase of the optimized structure for each density with respect to the minimum energy structure of each series.

Density / g cm^{-3}	RC model ΔE (eV)	SG model ΔE (eV)
0.7	0.00	0.48
1.0	0.60	0.00
1.5	5.76	1.04
2.0	29.06	13.37
3.0	27.73	80.86

4.3 Evaluation of graphitic content from IR spectra

Initial attempts by different groups to use IR spectra for the determination of the relative content of C sp^3 , sp^2 hybridization and H atoms in HAC samples, were based on a decomposition of the CH_x stretching band into various sub-bands associated with the aliphatic CH_2 and CH_3 groups and with aromatic CH. Literature band strengths from known aliphatic and aromatic molecules were then used for the evaluation of the sample composition. This procedure proved unreliable after inconsistencies were found in the comparison with results from other experimental techniques like nuclear magnetic resonance (NMR) or electric energy loss spectroscopy (EELS) (see discussion in Jacob and Möller²⁷). The main reason for the mentioned inconsistencies was the use of the IR absorption from CH stretching vibrations as the only source of information on aromatic structures, which excludes many of the C sp^2 atoms from polyaromatic structures.

More recently the possibility of extracting structural information on HAC samples from IR spectra alone has been revived in the astrophysical community,^{14,2} where IR spectra constitute the only observational data on interstellar dust. To that aim, the (weak) C=C band was also used in the evaluation in order to include the likely contribution of polyaromatic networks to the HAC structure. We have followed this procedure for the analysis of our experimental samples S1 and S2. The decomposition of the relevant absorption features into Gaussian bands is displayed in Fig. 5 and the assignment of the components is shown in Tables 3 and 4, respectively, together with the most recent absorption strengths of the different vibrational

modes, reported by Chiar *et al.*² In both cases there is a band at $\approx 1700\text{ cm}^{-1}$, which is most likely due to CO stretching attributable to sample contamination by very small amounts of CO, which is often found in plasma produced HAC.^{12,14} The very high oscillator strength of this CO band gives rise to an appreciable absorption even for very small CO abundance. In this work the CO mode is used for the decomposition of the band profile at $1800\text{-}1500\text{ cm}^{-1}$, but is not included in Tables 3 and 4.

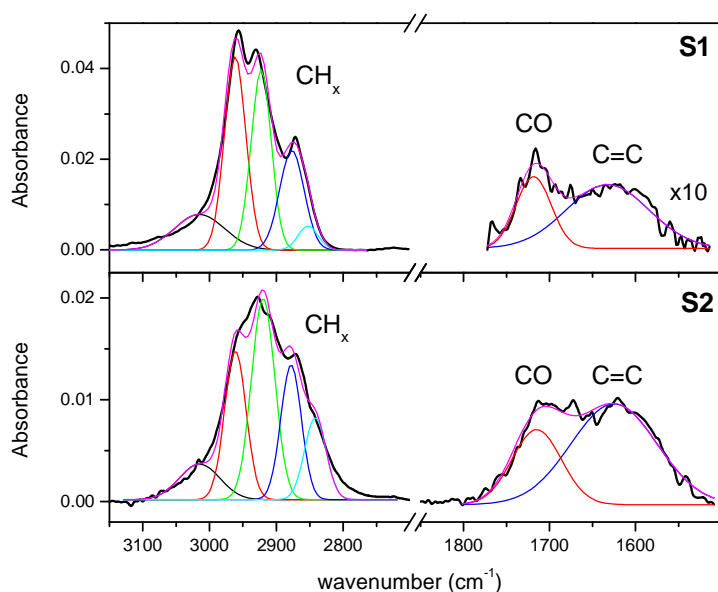


Fig. 5 (color online) Decomposition of the absorption bands relevant for the evaluation of the C sp^3 and sp^2 and H content of the experimental HAC samples S1 and S2. The thick black lines correspond to the experimental contours, and the pale pink contour is the sum of the components. For the assignment of the different Gaussians see text and Tables 3 and 4.

In comparison with the CH_x stretching absorptions at $\approx 2950\text{ cm}^{-1}$, the C=C stretching band at $\approx 1600\text{ cm}^{-1}$ is much more intense in S2 than in S1 and reflects the higher C/H ratio of the S2 sample, which suggests a larger polyaromatic content on this sample, as already advanced in the discussion of Fig. 3.

Table 3. Decomposition of band profiles for the S1 sample.

mode	Peak cm^{-1}	FWHM cm^{-1}	Area cm^{-1}	Band strength ^a $(\text{cm}^{-1}) \times 10^{18}$ ref 2
CH stretch arom	3015	88	0.74	2.58
CH_3 , a-stretch	2961	37	1.70	24.3
CH_2 , a-stretch	2922	35	1.50	15.2
CH_3 , s-stretch	2876	43	1.02	23.7
CH_2 , s-stretch	2852	35	0.20	14.8
C=C stretch	1632	113	0.14	0.275

^a Per group (CH , CH_2 , CH_3) except for the C=C stretch, which is given per C atom

Table 4. Decomposition of band profiles for the S2 sample

mode	Peak cm ⁻¹	FWHM cm ⁻¹	Area cm ⁻¹	Band strength ^a (cm ⁻¹)× 10 ¹⁸ Ref. 2
CH stretch arom.	3015	70	0.26	2.58
CH ₃ , a-stretch	2961	38	0.59	24.3
CH ₂ , a-stretch	2919	41	0.87	15.2
CH ₃ , s-stretch	2878	43	0.51	23.7
CH ₂ , s-stretch	2842	35	0.32	14.8
C=C stretch	1625	100	1.24	0.275

^a Per group (CH, CH₂,CH₃) except for the C=C stretch, which is given per C atom

For the derivation of the atomic composition of a given sample we have followed the same procedure as Chiar *et al.*² We have employed the asymmetric stretching bands of CH₃ and CH₂, the aromatic CH stretch, and the C=C stretch band. We have tacitly assumed that all H atoms are bonded to C sp³ or sp² bonds and have made no difference between olefinic and aromatic C=C bonds. The result of the evaluation is shown in table 5. We have also estimated the same magnitudes in our theoretical models by simply counting the appropriate atoms and bonds. The resulting values are listed in Tables 5 as well.

Table 5. Sample atomic composition from profile decomposition of experimental spectra and from HAC theoretical models. Samples have small (2nd and 3rd columns) and large (4th and 5th columns) polyaromatic content. The reproducibility in the experimental band intensities is typically 5-10%

	S1 profile decomposition	RC model	S2 profile decomposition	SG model
C sp ³	0.12	0.23	0.02	0.17
C sp ²	0.36	0.20	0.92	0.43
H	0.52	0.57	0.06	0.40

For HAC with small polyaromatic content (S1), the proportion of H atoms is high, both in the model and in the estimate from the experimental deposit; the Csp³/Csp² ratio, however is appreciably larger in the model. It is worth noting that in the RC model, many of the Csp² atoms are olefinic rather than aromatic. For HAC with a high polyaromatic proportion (S2) the differences between the model and the estimations from experiment are extreme. The relative content of C sp³, C sp² and H atoms derived from the band profile decomposition and the absorption strengths of Chiar *et al.*² points to a structure very close to that of graphite with just 6% of H atoms and more than 90% Csp² atoms, which is in stark contrast with the composition of the SG model structure (40% H atoms, 43% Csp² atoms).

5. Discussion

The actual structure of the experimental samples is not accurately known, but there is a reasonable similitude between the IR spectra of the HAC deposits and the model calculations

represented in Fig. 3. Consequently, it could be expected that the proportion of functional groups responsible for the IR absorptions of S1 and the RC model on the one hand, and between S2 and the SG model on the other hand, should be similar. However, Table 5 shows some striking disagreements, especially for the S2-SG data. In the following paragraphs we examine possible causes for such discrepancies in the atomic compositions reflected in Table 5.

The theoretical calculations have inherent limitations for the prediction of frequencies and line intensities, but we expect a reasonable agreement between experiment and theory, of the order of that found with the same method for polycyclic aromatic hydrocarbons (see Fig. 2), where the relative absorption between the CH stretching region around 3000 cm^{-1} and that below 1700 cm^{-1} , which includes bending vibrations and C=C stretchings, is reasonably well rendered by the method. The profile decomposition procedure illustrated in Fig. 5 has several problems. First of all, the theoretical calculations show that there is a substantial amount of mode mixing in the vibrations of the solid structure (see Table 1). The separation into isolated vibrational modes, inherent to the decomposition procedure, is thus just an approximation. Besides, there are some practical difficulties. Somewhat different sets of peak frequencies and bandwidths can lead to a satisfactory reproduction of the global profile. Baseline subtraction may introduce a large uncertainty in weak absorptions. Spurious lines, like the CO absorption at about 1700 cm^{-1} commented on above, can also complicate matters.

A key factor for the derivation of the atomic structure from the decomposition of the band profiles is the absorption strength value assumed for the various vibrations. In this work we have taken the values from Chiar *et al.*² These authors indicate that they have taken into account the effect of the carbon matrix, which makes their estimations preferable to previous literature values based on molecular data (see Chiar *et al.*², Dartois *et al.*¹⁴ and references therein). The pronounced influence of the local field on the absorption strength of the various functional groups is manifest in the strong dependence of the absorption spectra on density predicted by the theoretical calculations of the present work (see Section 3.2). Considering the fact that HAC denotes a type of material with a variable range of structures and densities, it is likely that different absorption strengths will correspond to a given vibration in different HAC solids and even to different parts of the same solid. Table 5 suggests that the set of absorption strengths used in the analysis leads to an overestimation of polyaromatic structures. This is particularly evident for the S2 HAC sample of the present work, where the C sp^3 , sp^2 and H fractions derived with the mentioned absorption strengths show an extreme preponderance of sp^2 atoms and are markedly different from the fractions of the SG model, which is unlikely given the similitude of their respective IR spectra (see Fig. 3). For the S1 HAC deposit, the composition derived from the experimental spectrum has also a higher C sp^2 fraction than that of the RC model, but in that case the absorption in the C=C region is much weaker and the discrepancy is smaller.

6. Astrophysical context

The CH_x stretching absorption feature of HAC around 2900 cm^{-1} ($3.4\text{ }\mu\text{m}$ band) is ubiquitously observed in the diffuse interstellar medium. This band alone does not allow an estimation of the aliphatic vs aromatic content of the material. The observation of weaker features requires large column densities and has been only possible in a few sources toward the galactic

center^{28,2} or in external galaxies.¹⁴ These weaker features include two peaks at 6.85 μm (1457 cm^{-1}) and 7.27 μm (1354 cm^{-1}) and a broader absorption band at $\approx 5.5\text{-}6.7 \mu\text{m}$ (1800-1500 cm^{-1}) which are also found in HAC. The peaks at 6.85 μm and 7.27 μm are assigned to a combination of CH_3 and CH_2 bendings and to a CH_3 bending respectively. The band at 5.5-6.7 μm has been discussed previously and is assumed to have contributions from olefinic and aromatic $\text{C}=\text{C}$ stretchings and probably from the stretching mode of CO . This weak, blended band is the only direct source of information on aromatic structures in the IR spectra of interstellar dust and, consequently, estimates of the aromatic vs aliphatic content of carbonaceous dust grains are subject to a large uncertainty.

The absorption spectrum of the IRAS 08572+3915 galaxy in the 3.4 μm band and in the $\approx 5.5\text{-}8 \mu\text{m}$ interval is represented in Fig. 6, together with the calculated spectra of the two theoretical models studied in the present work. Absorption spectra of the same regions towards the Galactic center,^{28,2} differ somewhat depending on the specific source, but the relative absorption intensities between the 3.4 μm band and the absorption features in the 5.5-8 μm region are comparable to those of IRAS 08572+3915.

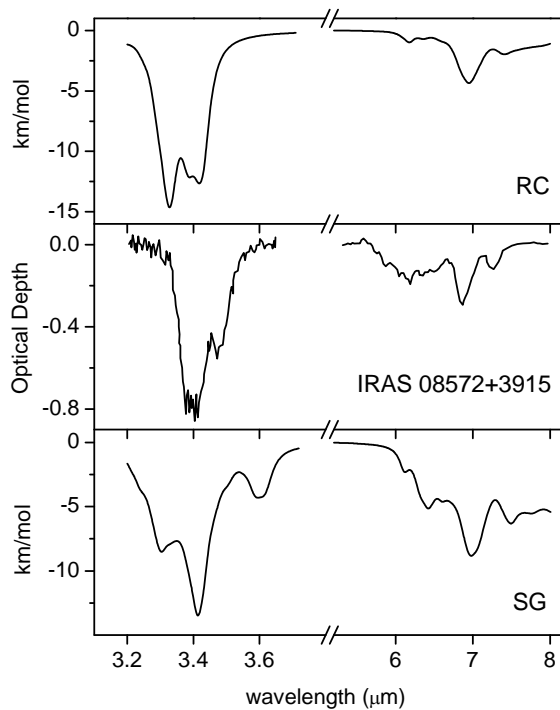


Fig. 6 Comparison of calculated and astronomical spectra. Upper panel: H-rich RC model. Middle panel: Observed spectrum from the IR galaxy IRAS 08572+3915 (from ref. 14). Lower panel: Spectrum of graphitic-rich SG model.

The observed spectra have been used by various authors to infer details on the structure and composition of interstellar carbonaceous dust. Chiar *et al.*² analyzed IR absorption spectra from sources toward the galactic center and used the profile band decomposition and absorption strengths that we have adopted in the present work (see section 3.3). From this

analysis they concluded that Galactic hydrocarbon dust has, on average, a low H/C ratio and sp^3 content and is highly aromatic. However, as discussed in the previous section, this analysis seems to be biased toward highly polyaromatic structures. In addition the results of the present work show that in the IR spectra of polyaromatic HAC solids the characteristic aliphatic bending modes at $6.85 \mu\text{m}$ (1557cm^{-1}) and $7.27 \mu\text{m}$ (1354cm^{-1}) stand out on top of a broad and intense absorption band (see Fig. 6), whereas only comparatively weak absorption peaks are found at these frequencies in the observations.²⁸ This discrepancy and the worse reproduction of observed spectra in the $3.4 \mu\text{m}$ band region, suggest that the average molecular structure for hydrocarbon dust proposed by Steglich *et al.*¹⁶ and used as basic unit for the SG model, might not be adequate when incorporated into an amorphous solid.

In a previous work Dartois *et al.*¹⁴ studied IR absorptions of carbonaceous dust in the infrared Galaxy IRAS 08572+3915. From a comparison of the observed spectra with laboratory HAC samples generated under soft conditions, and through the application of astronomical constraints and network bond models, these authors concluded that interstellar carbonaceous dust is a hydrogenated solid dominated by an aliphatic/olefinic backbone structure, consistent with the basic structure of the RC model used in the present work.¹¹ Dartois *et al.*¹⁴ did not fit the CH and C=C bands in the observed spectra, but set only upper limits to these absorptions. The spectra of aromatic-poor HAC solids like those represented by the RC model are in better global agreement with astronomical observations over the $3.2\text{-}7.7 \mu\text{m}$ ($3100\text{-}1300 \text{cm}^{-1}$) range^{28,14,2} (see Fig. 6), but the peaks in the $5.7\text{-}7.4 \mu\text{m}$ ($1750\text{-}1350 \text{cm}^{-1}$) interval, and in particular in the $\approx 6\text{-}6.4 \mu\text{m}$ ($1680\text{-}1550 \text{cm}^{-1}$) interval, corresponding to C=C stretching vibrations, are too weak as compared with the $3.2\text{-}3.63 \mu\text{m}$ ($3100\text{-}2750 \text{cm}^{-1}$) absorption band. An average structure with an aromatic content intermediate between those of Dartois *et al.*¹¹ and Steglich *et al.*,¹⁶ possibly closer to that of Dartois *et al.*¹¹, would probably provide a better description of the observations.

7. Conclusions

We have developed ab initio theoretical models of amorphous structures for two of the current kinds of arrangements proposed for HAC particles of astrophysical relevance, one with a large graphitic core with substituents, model SG, and another one with small aromatic islands and hydrocarbon chains, but without any substantial graphitic content, model RC. We have generated hydrogen-rich and graphitic-rich HAC deposits in our laboratory using PECVD of CH_4/He mixtures. A reasonably good agreement is achieved between the IR spectra of the experimental samples and those of the theoretical models. Based on our calculations, we can put forward an assignment for the main features in the observed spectra. These assignments add further information to previous literature designations.

Our calculations for varying density values show the large effect of the local environment on the absorption strength of a given vibrational mode and send a word of caution about the line strengths to be used for the estimate of sample compositions. The model densities yielding spectra in best agreement with the experimental samples are somewhat lower than those currently estimated in the literature for the HAC materials considered.

We show that the method usually employed to determine the relative content of various types of C bonding and H content can induce significant misidentifications, as it is based on the

measurement of band intensities often blended with other modes and on absorption strengths that may not be adequate for these solids. In contrast, comparison with theoretical models where the C and H content is straightforward, can offer semi-quantitative values for the corresponding magnitudes.

Finally, comparison of our models with astrophysical observations suggests that the carriers of the IR absorption bands in the interstellar medium should not have a predominantly hydrogen-poor graphitic structure, as reported in recent works, but contain, besides aromatic rings, a significant hydrogen-rich aliphatic fraction.

Future work along this line will incorporate improvements on the theoretical models, like e.g. by including heteroatoms in the structures, or establishing links among polyaromatic sheets.

Acknowledgments

This work has been funded by the MINECO of Spain under grant FIS2013-48087-C2-1P, by the MICINN of Spain under grant CDS2009-00038, and by the European project ERC-2013-SyG, Grant Agreement 610256 "NANOCOSMOS". G.M acknowledges MINECO PhD grant BES-2014-069355. Our skillful technicians M.A. Moreno, A. González and J. Rodríguez are also gratefully acknowledged.

References

1. A. P. Jones, L. Fanciullo, M. Köhler, L. Verstraete, V. Guillet, M. Bocchio, and N. Ysard, *Astron. Astrophys.* 2013, 558, A62.
2. J. E. Chiar, A.G. G.M. Tielens, A. J. Adamson, and A. Ricca, *Astrophys. J.* 2013, **770**, 78.
3. W. W. Duley and D. A. Williams, *Mont. Not. R. Astr. Soc.* 1983, 205, 67
4. A. P. Jones, W. W. Duley and D. A. Williams, *Q. Jl. R. astr. Soc.*, 1990, 31, 567.
5. J. Robertson, *Adv. Phys.* 1986, 33, 317
6. J.C. Angus and F. Jansen, *J. Vac. Sci. Technol. A.* 1988, 6, 1778.
7. W. Jacob, *Thin solid films*, 1998, 326, 1.
8. J. Robertson, *Mat. Sci. Eng. R.*, 2002, **37**, 129
9. Y. J. Pendleton and L. J. Allamandola, *Astrophys. J. Suppl. Ser.* 2002, 138, 75
10. C. Jäger, S. Krasnokutsky, A. Staicu, F. Huisken, H. Mutschke, Th Henning, W. Poppitz, and I. Voicu, *Astrophys J. Suppl. Ser.* 2006, 166, 557.
11. E. Dartois, G. M. Muñoz-Caro, D. Deboffle, G. Montagnac, and L. d'Hendecourt, *Astron. Astrophys.* 2005, **432**, 895
12. E. Kovacevic, I. Stefanovic, J. Berndt, Y. J. Pendleton and J. Winter, *Astrophys J.*, 2005, 623, 242
13. B. Maté, I. Tanarro, M. A. Moreno, M. Jiménez-Redondo, R. Escribano, and V. J. Herrero, *Faraday Discuss.* 2014, **168**, 267.
14. E. Dartois, T. R. Geballe, T. Pino, A. T. Cao, A. Jones, D. Deboffle, V. Guerrini, Ph. Bréchingac, and L. d'Hendecourt, *Astron. Astrophys.* 2007, **463**, 635.
15. S. Kwok and Y. Zhang, *Astrophys. J.*, 2013, 771, 5.

16. M. Steglich, C. Jäger, F. Huisken, M. Friedrich, W. Plass, H.-J. Räder, K. Müllen, and Th. Henning, *Astrophys. J. S.* 2013, **208**, 26
17. V. Timón, O. Gálvez, B. Maté, I. Tanarro, V.J. Herrero and R. Escribano, *Phys.Chem.Chem.Phys.* 2015, **17**, 28966-76.
18. R. L. C. Akkermans, N. A. Spenley, and S. H. Robertson, *Molec. Simul.* 2013, **39**, 1153.
19. S. J. Clark, M. D. Segall, C. J. Pickard, P. J. Hasnip, M. J. Probert, K. Refson and M. C. Payne, *Z. Krist.*, 2005, **220**, 567–570.
20. K. Refson, P. R. Tulip and S. J. Clark, *Phys. Rev. B*, 2006, **73**, 155114.
21. J. P. Perdew, K. Burke, M. Ernzerhof, D. of Physics and N. O. L. 70118 J. Quantum Theory Group Tulane University, *Phys. Rev. Lett.*, 1996, **77**, 3865–3868.
22. S. Grimme, *J. Comput. Chem.*, 2006, **27**, 1787.
23. NIST Chemistry WebBook, NIST Standard Reference Database Number 69, Eds. P.J. Linstrom and W.G. Mallard, National Institute of Standards and Technology, Gaithersburg MD, 20899
24. B. Maté, G. Molpeceres, M. Jiménez-Redondo, and I. Tanarro, *Astrophys J.* 2016 (in press).
25. T. Schwarz-Selinger, A. von Keudell, and W. Jacob, *J. Appl. Phys.* 1999, **86**, 3988.
26. L. J. Allamandola, S. A. Sandford, A. G. G. M. Tielens, and T. M. Herbst, *Astrophys. J.* 1992, **399**, 134
27. W. Jacob and W. Möller, *Appl. Phys. Lett.*, 1993, 63, 1171.
28. J. E. Chiar, A. G. G. M. Tielens, D. C. B. Whittet, W. A. Schutte, A. C. A. Boogert, D. Lutz, E. F. van Dishoeck, and M. P. Bernstein, *Astrophys. J.* 2000, 537, 749.